2014 年 8 月
博士學位論文
論文

Synthesis and physico-chemical characteristics of β-Tricalcium Phosphate from abalone shell

朝鮮大學校 大學院

齒醫生命工學科

朴 正 剛

2014年 8月 博士學位論文 전복 패각을 이용한 베타 제삼인산칼슘의 합성 및 물리화학적 특성

박 정 강

전복 패각을 이용한 베타 제삼인산칼슘의 합성 및 물리화학적 특성

Synthesis and physico-chemical characteristics of β-Tricalcium Phosphate from abalone shell

2014年 8月 25日

朝鮮大學校 大學院

齒醫生命工學科

朴 正 剛

Synthesis and physico-chemical characteristics of β-Tricalcium Phosphate from abalone shell

指導敎授　金　秀　官

이 論文을 齒醫學博士學位신청 論文으로 提出함.

2014年　4月

朝鮮大學校 大學院

齒醫生命工學科

朴　正　剛

朴正剛의 博士學位論文을 認准함

委員長　　首爾大學校　敎　授　이 종 호 印

委　員　　朝鮮大學校　敎　授　임 성 철 印

委　員　　朝鮮大學校　敎　授　이 숙 여 印

委　員　　朝鮮大學校　敎　授　김 재 성 印

委　員　　朝鮮大學校　敎　授　김 수 관 印

2014年　6月

朝鮮大學校 大學院

CONTENTS

LIST OF FIGURES ····· iii
LIST OF ABBREVIATIONS ····· iv
ABSTRACT ····· V

Ⅰ. Introduction ····· 1
Ⅱ. Materials and methods ····· 6
Ⅱ-A. Materials ····· 6
Ⅱ-B. The process of β-TCP synthesized from abalone shell ····· 7
Ⅱ-B-1. Preparation of abalone shell to synthesize calcium oxide ····· 7
Ⅱ-B-2. Synthesis of Calcium oxide from abalone shell ····· 7
Ⅱ-B-3. Synthesis of Calcium carbonate from calcium oxide derived from abalone shell ····· 8
Ⅱ-B-4. Synthesis of Dicalcium phosphate ····· 8
Ⅱ-B-5. Synthesis the TCP from DCP ····· 9
Ⅱ-B-6. Physical and Chemical analysis of synthesized β-TCP from abalone shell ····· 10
Ⅱ-C. The biological safety assessment ····· 11
Ⅱ-C-1. Cell viability (MTT assay) ····· 11
Ⅱ-C-2. Cell survival assay ····· 11
Ⅲ. Results ····· 13
Ⅲ-A. Characterization of the abalone shell transformed to CaO by sintering at different temperatures ····· 13
Ⅲ-B. The synthesis of $CaCO_3$ from abalone shell-derived CaO using CO_2 immit method ····· 15

Ⅲ-C. Identification of optimize pH to synthesize the DCP from abalone shell-derived $CaCO_3$ 17
Ⅲ-D. Synthesis of β-TCP from abalone shell-derived DCP 20
Ⅲ-E. SEM images and EDS analysis of the β-TCP synthesized from abalone shell 25
Ⅲ-F. The cell cytotoxicity of β-TCP synthesized from abalone shell 27
Ⅲ-G. Cell survival assay 29
Ⅳ. DISCUSSION 31
Ⅴ. REFERENCES 36

감사의 글 43

LIST OF FIGURES

Figure 1. Schematic diagram of β-TCP synthesized from abalone shell 6

Figure 2. Identification of optimal temperature to synthesize CaO from abalone shell 14

Figure 3. FT-IR analysis to verify the synthesis of $CaCO_3$ from abalone shell-derived CaO by CO_2 gas-infusing 16

Figure 4. FT-IR analysis of DCP obtained at different pH to determine a valid pH 18

Figure 5. XRD analysis of DCP synthesized at 6.02 pH compared with control DCP 19

Figure 6. FT-IR analysis of β-TCP sintered at different temperatures to determine a valid sintering temperature 21

Figure 7. XRD analysis of the β-TCP synthesized from TCP sintered at 1050℃ compare with control β-TCP..... 22

Figure 8. Reaffirmed of β-TCP synthesized from abalone shell by the Korea Institute of Ceramic Engineering and Technology (Seoul, Republic of Korea) measured by XRD 23

Figrue 9. SEM images showing surface appearance of β-TCP sheets 25

Figure 10. EDS analysis of β-TCP synthesized from abalone shell 26

Figrue 11.Cell viability of β-TCP synthesized from abalone shell 28

Figure 1. Comparison of cell survival between commercial β-TCP used as control β-TCP synthesized from abalone shell 30

LIST OF ABBREVIATIONS

GBR	Guided bone regeneration
HA	Hydroxyapatite
β-TCP	Beta tricalcium phosphate
TCP	Tricalcium phosphate
MFDS	Ministry of Food and Drug Safety
NiFDS	National Institute of Food and Drug Safety Evaluation
FBS	Fetal Bovine Serum
DMEM	Dulbecco's Modified Eagle's Medium
HNOKs	Human normal oral keratinocytes
MG63	Human MG63 osteosarcoma cells
MTT	3-(4, 5-dimethylthiazolyl-2)-2, 5-diphenyltetrazolium bromide
DMSO	Dimethyl Sulfoxide
DAPI	4',6'-diamidino-2-phenylindole dihydrochloride
DPBS	Dulbecco's phosphate-buffered saline
SEM	Scanning Electronic Microscopy
EDS	Energy Dispersive X-ray Spectrometer
XRD	X-ray Diffractometer
FT-IR	Fourier-transform infrared spectroscopy

ABSTRACT

Synthesis and physico-chemical characteristics of β-Tricalcium Phosphate from abalone shell

ZHENGGANG PIAO

Advisor: Prof. Su-Gwan Kim D.D.S., Ph.D.

Department of Bio Dental Engineering,

Graduate School of Chosun University

치주질환을 비롯한 다양한 원인으로 유도되어지는 골 소실의 치료 및 시술 방법으로는 소실된 치조골의 골 결손부를 치은 조직이 덮지 못 하도록 다양한 종류의 골 이식재를 사용하여 시행되어지는 골 이식술(Bone grafting) 및 골유도 재생술(Guided bone regeneration, GBR) 등이 있다. 이는 골 이식재가 임플란트와 치주 조직 간의 결합력을 향상시켜 골 재생 효과를 높여주고, 골 이식재로 메워진 골 결손부의 신생골 형성에 효과적이기 때문이다. 이러한 골 이식술이 기능적 뿐만 아니라 심미적 기능으로 보편화됨에 따라 수술 및 시술에 앞서 골 결손부의 잔존 골량이 부족한 경우를 대비한 다양한 종류의 골 이식재 중 장단점을 고려하여 자신에게 맞는 골 이식재를 선택하는 것 또한 중요한 치료 요소로 꼽히고 있다. 현재까지 많은 타입의 합성생체재료로 제작된 이식재가 많이 연구 되고 있다. 베타 삼 인산칼슘 (β-TCP) 는 훌륭한 생체재

료로서 골 재생에 좋은 효과를 보이고 있다.

본 연구의 목적은 전복 패각에서 효율이적이고 생체안정성이 좋은 β-TCP (beta Tricalcium Phosphate)를 제조하는 과정 및 고 순도의 β-TCP를 제작하여 이식재의 합성재료로서의 생체적합성 및 안정성을 한국 식품 의약품 안전처 (Ministry of Food and Drug Safety, MFDS)와 한국 식품의약품 안전평가원 (National Institute of Food and Drug Safety Evaluation, NiFDS) 에서 제공한 의료기기 평가가이드라인에 의거하여 생물학적, 물리·화학적 특성을 분석하여 골 이식 시 예견성이 좋고, 효율적이며 경제적인 합성 골 이식재를 합성할수 있는 생체재료로서의 각각의 특성을 평가하고자 하였다.

전복 패각을 수거하여 삼차 증류수 및 과산화수소로 여러번 세척하여 패각에 붙은 이물질을 제거하였다. 깨끗이 세척된 전복 패각을 950℃에서 소결하여 산화칼슘을 제작하였고 얻어진 산화칼슘은 물과 반응하여 수산화칼슘용액으로 만들고 이산화탄소 주입 방법을 이용하여 탄산칼슘 침전 용액을 만들었다. 탄산칼슘 침전용액은 여과지로 여과하여 70℃에서 10시간 건조하여 고순도의 탄산칼슘 분말을 제조하였다. 제조된 탄산칼슘은 10% 인산용액과 반응하여 침전이 일어나게 한 다음 얻어진 침전물을 수세 및 여과과정을 거친 후 70℃에서 10시간 건조하여 고순도 인산1수소칼슘 분말을 제조하였다. 제조된 인산1수소칼슘 분은 산화칼슘과 몰 반응을 하여 삼 인산칼슘을 제조하였고 수세, 여과 및 건조과정을 거쳐 고 순도 삼인산칼슘분말을 제조하였다. 제조된 삼인산칼슘분말을 1150℃에서 소결하여 고 순도 베타 삼인산칼슘분말을 제작하였다.

전복 패각으로부터 만들어진 고 순도 베타 삼 인산칼슘의 물리화학적 특성은 주사현미경을 이용하여 표면분석, Ca/P 비율 분석 및 결정상 분석을 하였으며 비율이 1.91로 확인 되었으며 용출된 고농도의 칼슘이 용출과정에 의해 희석되어짐에 따라 구강 정상세포(hNOKs)와 인체 조골세포(MG-63) 모두에서 높은 세포안정성을 나타내었다.

Ⅰ. Introduction

Modern society has being rapidly moved to aging society by the extension of life expectancy due to advancing economic development and medical science. For this reason, elderly patient with requiring dental implant placement caused by various oral disease have being explosively increased in dentistry. However, for increasing the success rate of dental implant placement, the recipient site need to sufficient bone volume and quality [1]. Whereas, patient with requiring dental implant placement usually have an insufficient bone volume and a low quality bone caused by exelcymosis, bone resorption, periodontal defects or trauma. Therefore, guided bone regeneration (GBR) is performed clinically using bone grafting materials for increasing the volume and quality of bone at the recipient site [2-4].

Presently, bone graft materials are classified as four divisions according to the its basic compounds : autogenous, allograft, alloplast, and xenograft. The ideal bone graft materials has always been autogenous bone, which is derived from the individual for whom the bone graft is intended. Even though autogenous bone can permit the excellent predictability and have osteogenesis, osteoinduction, and osteoconduction with bio-compatability and biological safety, it need to harvest from the surgical patient from whom a second surgical wound site must be used. [5-7]. Although autologous bone graft have a major disadvantage, it offers the promise of high levels of success while avoiding the possibilities of antigenicity [8-12]. Allografts are tissues taken from individuals of the same species as the hosts. A major advantage of allograft is that the materials can without the requirement of a secondary surgery to harvest the bone at other site. While, disadvantages are that the materials prepared from cadaver or donor have a cultural taboos, social ethics, and antigenicity [13-19]. Xenografts are derived from other species. It is need to totally remove the their organic components to avoid

the immunological reactions becomes nonexistent. Because the inorganic materials maintains the physiological dimension of the augmentation during the remodeling phases. Therefore, alloplastic bone graft materials guaranteed with biological safety have became noted [20-22]. Alloplasts are synthetic bone graft materials which contribute to the repair of defective bone and to the enhancement of bone ingrowth [23, 24]. Today, with the use of synthetic bone graft materials composed of bioceramic tricalcium phosphate and hydroxyapatitie, it is possible to enhance the volume, width, and height of bone in deficient areas to regenerate the bone supporting implant replacement [25-28].

Calcium phosphates have been evaluated as potential materials for bone tissue engineering. Calcium phosphate materials are similar to bone in composition and have bioactive and osteocondutive properties. Calcium phosphate materials show a positive interaction with living tissue, which includes the differentiation of immature cells towards bone cells [29, 30]. Tricalcium phosphate exists in many polymorphs (α, β, ɣ, and super-α) [31]. Only two polymorphs (α and β) are used as biomaterials [32]. These phases have attracted considerable attention and a range of bone graft materials have been manufactured and used widely in clinical practice. The advantages of calcium phosphates are they can be injected directly into a bone defect and set in situ. In addition, they are biocompatible and resorbable [33, 34]. Among these materials, the most prevalent is over come. β-TCP has the properties of high biocompatibility an osteoconductivity [35, 36]. because of these features, β-TCP leads to bone apposition in the areas contacting with the material [37].

Although various kinds of synthetic bone grafting materials based on β-TCP has been developed for using the GBR, but these have a highly expensive due to the complicated synthesis process. Therefore, an economic and efficient synthesis of β-TCP process should be developed.

Recently, biocompatible β-TCP powders was synthesized from natural materials, such as eggshells, cuttlefish bone and oyster shell [38]. But, it is difficult to be recycled and these shells contain mass protein. Contrary, abalone shells were easy to recycled because of the vast majority of them are discarede as rubbish. And then, abalone shells contain very little of protein. So that, it is easily synthesis to high purity of biocompatible source as $CaCo_3$ for synthesize high purity of β-TCP powders. On the other hand, many studies used complex process, high level concentration and several kind of acid to reaction for synthesize β-TCP. However, In this study, during the synthesize β-TCP based on the abalone shell processes were only using CO_2 immit method, 10% phosphor acid to phosphor reaction and sintering process. These development of processing technology could be increase of biocompatible and biological safety of β-TCP synthesized from abalone shell.

Although abalone shells largely consist of nacre which is a composite structure conposed of aragonitic calicum carbonate, but it is regarded as an industrial waste due to its excellent bulk mechanical properties more than other shells. But, abalone shell is exceptionally strong and is comprised of microscopic calcium carbonate tiles stacked like bricks. A large number of abalone had used in several industries. The meat (foot muscle) of abalone is used for food, and the shell is used as decorative items and as a source of jewelry, buttons, buckles and inlays, but the vast majority of them are discarded as rubbish and are environmental pollutants [39]. Every year, the tipping fees for the proper disposal of waste abalone shell are particularly high. Therefore, industries related with abalone farm need to develop the processing technology for preventing the marine pollution caused by the waste of abalone shell and for creating the high value added product based on the abalone shell.

The aim of this study was to develop the processing technique to synthesis the biocompatible bioceramic β-TCP from abalone shell and to evaluate the physico-chemical characteristics of β-TCP synthesized from abalone shell. In this study, the experiment conformed to the Ministry of Food and Drug Safety, (MFDS) and National Institute of Food and Drug Safety Evaluation, (NiFDS) furnished guidelines for an evaluation of the biological and physicochemical characteristics.

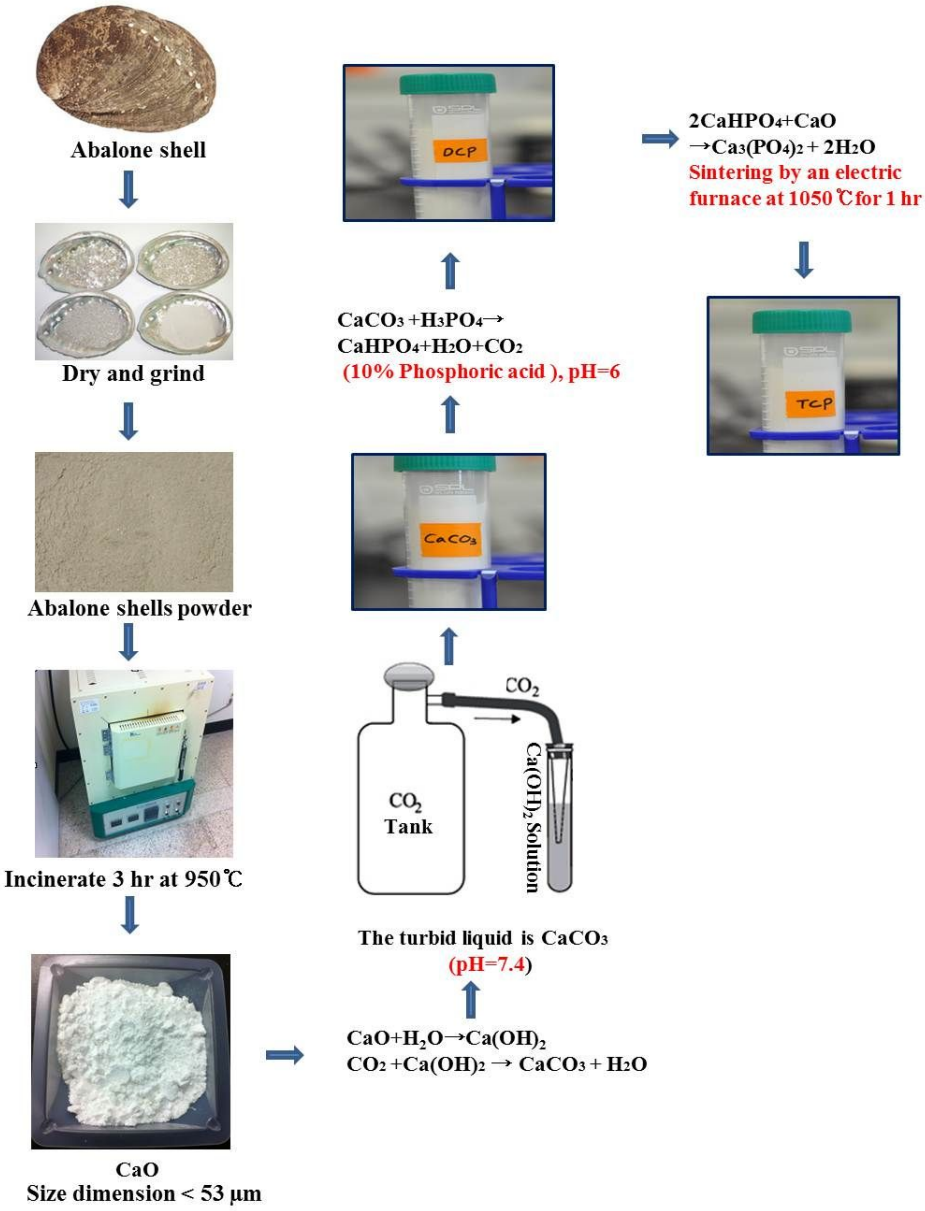

Figure 1. Schematic diagram of β-TCP synthesized from abalone shell

Ⅱ. MATERIALS AND METHODS

Ⅱ-A. Materials

Abalone shells (WD, Republic of Korea) was used in this study were collected the near ocean of wando, Republic of Korea. As the control ceramics, Calcium oxide (CaO) were purchased from DaeJung Co. (DG, Republic of Korea). Calcium carbonate ($CaCO_{3)}$ were purchased from Sigma-aldrich Co. (MO, USA). Dicalcium phosphate (DCP, $CaHPO_4$) and β-TCP ($Ca_3(PO_4)_2$, ASSAY min. 99.9%) were purchased from OssGen (GB, Republic of Korea) and Georgiachem (Atlanta, GA, USA), respectively.

For the analysis of cell viability and survival, Human MG-63 osteosarcoma cells was purchased from Korea cell line bank (KCLB, Seoul, Republic of Korea), and human normal oral keratinocytes (hNOKs) was purchased from ScienCell Reseach Laboratories (Carlsbad, CA, USA). Fetal bovine serum (FBS), Dulbecco's phosphate-buffered saline (DPBS), Dulbecco's modifed Eagles' medium (DMEM), penicillin, and streptomycin were purchased from Gibco (NY, USA). MTT (3-(4, 5-dimethylthiazol-2-yl)-2, 5-diphenyl tetrazolium bromide) and dimethylsulfoxide (DMSO) were purchased from Sigma-aldrich Co. (MO, USA). 4'6'-diamidino-2-phenylindole dihydrochloride (DAPI) and LIVE/DEAD® Reduced Biohazard Cell Viability Kit were purchased from Invitrogen (NY, USA).

Ⅱ-B. The process of β-TCP synthesized from abalone shell

The processing steps to synthesize the β-TCP from abalone shells were briefly described in Fig. 1.

Ⅱ-B-1. Preparation of abalone shell to synthesize calcium oxide

As the washing step to synthesize the calcium oxide, contaminants attached on the balone shells were removed by distilled water in Ultrasonicator (KODO, JAC-4020, Republic of Korea) for 30 min at room temperature an repeated this step five times. Sequentially, abalone shells were incubated in gydrogen peroxied hydrogen peroxide (Duksan,, Republic of Korea) in an ultrasonicator for 100 min fo remove the remained contaminants and to sterilze. The abalone shells were washed by distilled water using an ultrasonicator for 100 min. Finally, the abalone shells were dried at room temperature for 2 days.

Ⅱ-B-2. Synthesis of Calcium oxide from abalone shell

Completely dried abalone shells were pulverized using a powder in a blender. To synthesize the calcium oxide, pulverized abalone shells were sintered by an electric furnace at 950℃ (the temperature was increased 100℃/hr) for 3 hr. After sintering,

residue with 〉53 μm particle size were collected by fine silt. Sequentially, purity and synthetic rate of calcium oxide from abalone shell were evaluated by FT-IR and XRD analysis

Ⅱ-B-3. Synthesis of Calcium carbonate from calcium oxide derived from abalone shell

Calcium oxide derived from abalone shell was dissolved in deionized water by stirring with a magnetic bar at 250 rpm. After calcium oxide was completely safurated as calcium hydroxide ($Ca(OH)_2$), the CO_2 gas was infused into the $Ca(OH)_2$ solution by pH 7.4.

$$CaO + H_2O \rightarrow Ca(OH)_2$$

$$Ca(OH)_2 + CO_2 \rightarrow CaCO_3$$

Produced residues products were rinsed three times by distilled water to remove the impurities, filtered through filter paper, and dried in dry oven controlled at 70℃ for 24 hr. Sequentially, purity and synthetic rate of calcium hydroxide from abalone shell were evaluated by FT-IR and XRD analysis

Ⅱ-B-4. Synthesis of Dicalcium phosphate (DCP)

Calcium carbonate was dissolved in deionized water by stirring with a magnetic bar at 200 rpm. After stirring, a 10% phosphoric acid was added drop-wisely to into calcium carbonate dolution by pH 6.0.

$$CaCO_3 + H_3PO_4 \rightarrow CaHPO_4 + H_2O + CO_2$$

Produced residues products were rinsed three times by distilled water to remove the impurities, filtered through filter paper, and dried in dry oven controlled at 70℃ for 24 hr. Sequentially, purity and synthetic rate of DCP from abalone shell were evaluated by FT-IR and XRD analysis.

Ⅱ-B-5. Synthesis the TCP from DCP

Synthesized DCP was dissolved in deionized water by stirred with a magnetic bar at 200 rpm. After stirring, the CaO was added drop-wisely into the DCP solution to synthesize the TCP.

$$2CaHPO_4 + CaO \rightarrow Ca_3(PO_4)_2 + 2H_2O$$

The impurities were removed by filtration and rinsing several times with deionized water. The suspension was filtered and then dried in dry oven controlled at 70℃ for 24 hr. Remain residues were sintered by an electric furnace (MF-22G, JEIO TECH) at 950℃ ~ 1100℃ (the temperature was increased by 100℃/hr) for 3 hr to synthesize the β-TCP. Sequentially, purity and synthetic rate of β-TCP from abalone shell were evaluated by FT-IR and XRD analysis.

Ⅱ-B-6. Physical and Chemical analysis of synthesized β-TCP from abalone shell

The morphology was observed by scanning electron microscopy (SEM; JSM 840-A, JEOL co., Japan). The chemical characteristics were measured by Fourier-transform infrared (FT-IR; Nicolet 6700, Thermo Electron, USA) spectroscopy. The crystal structure of the materials was determined by X-ray diffraction (XRD, X'Pert PRO MRD, PAN alytical co. The Netherlands) using Cuk_a radiation produced at 40 kV and 30 mA. The patterns were scanned from 10° ~ 60° 2Θ at a scan rate of 2° per minute with a step size of 0.05°. The Ca/P ratio was examined by energy dispersive X-ray (EDS, XS-169, Japan) spectrometry. The physical and chemical characteristics of the synthesized materials were analyzed according to the MFDS (the Ministry of Food and Drug Safety) guidelines.

Ⅱ-C The biological safety assessment

Ⅱ-C-1. Cell viability (MTT assay)

Human MG-63 osteosarcoma cells (KCLB, Korea cell line bank, Seoul, Republic of Korea) and human normal oral keratinocytes (hNOKs) were cultured in DMEM medium supplemented with 10% FBS and 1% penicillin/streptomycin in humidified atmosphere containing 5% CO_2 at 37℃. The cell viability was assessed using a MTT (3-(4, 5-dimethylthiazol-2-yl)-2, 5-diphenyl tetrazolium bromide) assay.

The control β-TCP and abalone shell β-TCP were released in 10% FBS solution for 3 times at 72 hr. Thereafter, 20 μL of solution was added to 1 mL culture medium to each well and the incubated at 37°C for 4 hr. Afterthat, 200 μL dimethylsulfoxide (DMSO) was added after supernatant medium was removed. Finally, solution was transferred into the 96-well plate and the absorbency value was recorded 540 nm (Epoch Micro-volume Spectrophotometer System, BioTek, VT, USA).

Ⅱ-C-2. Cell survival assay

The cell attachment of the control β-TCP and abalone shell β-TCP was assessed using a modified 4'6'-diamidino-2-phenylindole dihydrochloride (DAPI) stain and live and dead cell viability assay. 25 mg of the control β-TCP and abalone shell β-TCP were add to a 24-well, respectively, which was followed by the addition of human MG-63 cells and human normal oral keratinocytes

(hNOKs). Finally, 5×10^5 of the cells was added to the 24-well plate in a humidified at mosphere containing 5% CO_2 at 37℃.

For the DAPI stain experiment, the cells were washed twice with 1X Dulbecco's phosphate-buffered saline (DPBS) after removing the supernatant medium. The fixation solution was 4% paraformaldehyde at 15 min. The cell attachment morphology was observed by fluorescence microscopy (Eclipse TE200; Nikon Instruments, NY, USA) after washing twice with a DPBS solution.

LIVE/DEAD® Reduced Biohazard Cell Viability Kit (Invitrogen, NY, USA) was used according to the manufacturer's protocol.

Ⅲ. Results

Ⅲ-A. Optimize sintering temperature to synthesize the CaO from abalone shell

To identify the optimize sintering temperature to synthesize the CaO. The CaO, paralited abalone cells were sintered by an electric funace at 900℃, 950℃ and 1000℃, respectively. After sintering at different temperature synthesized residues were performed FT-IR to verify the CaO synthesis from abalone shells.

As shown in Fig. 2, FT-IR analysis of the residues sintered at 900℃, 950℃ and 1000℃ showed a sharp band at 3656 cm^{-1}, two broad weak bands centered at approximately 3822 and 3388 cm^{-1}, a medium doublet centered at around 1444 cm^{-1}, and a very strong absorption below 600 cm^{-1}. Especially, Fig. 2B shows that all the absorptions displayed for CaO are similar to those exhibited by commerial CaO. CaO has a broad band between 250 and 600 cm^{-1} corresponding to the stretching vibration of the Ca-O group. These data is indicating that optimize sintering condition to synthesize CaO form for abalone shell is sintered at 950℃ for 3 hr.

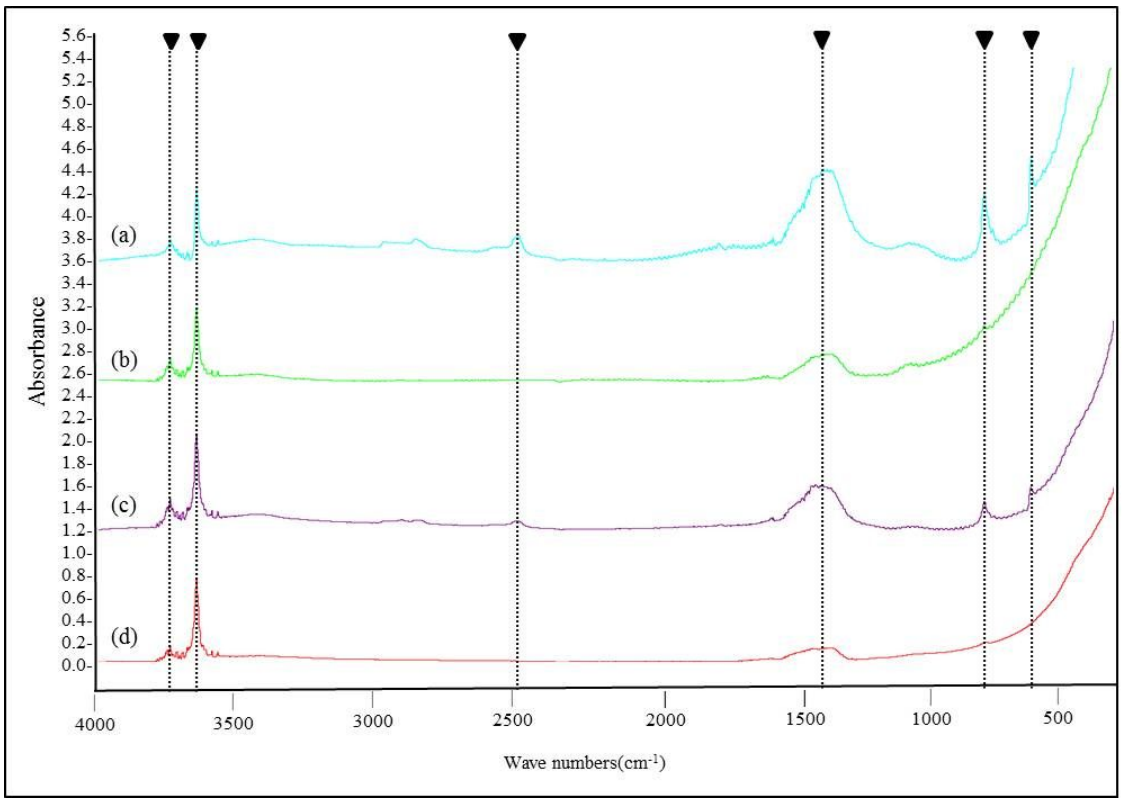

Figure 2. Identification of optimal temperature to synthesize CaO from abalone shell. Each residues synthesized at different temperature were performed the FT-IR analysis to verity the synthesis of CaO from abalone shell. (a) commercial CaO, abalone shell sintered at (b) 900℃, (c) 950℃ and (d) 1000℃. As shown the Fig. 2, sintered at 950℃ seemed to the most similar peak compared with control Cao. Black arrow indicate the matching pick compared with commercial CaO used as control.

Ⅲ-B. The synthesis of $CaCO_3$ from abalone shell-derived CaO using CO_2 immit method

To evaluate the synthesis of $CaCO_3$ from abalone shell-derived CaO, residues synthesized by modified CO_2 immit method were performed FT-IR analysis. As shown in Fig. 3, the integrated carbonate bands between 2646 - 2423 cm^{-1}, 1833 - 782 cm^{-1} and 930 - 730 cm^{-1}. The fraction of $CaCO_3$ present by integrating the bands at various wave numbers relative to the intensity in the same region of the spectrum of the commercial $CaCO_3$ used as control. Therefore, this data is demonstrated that, $CaCO_3$ was successfully synthesized from abalone shell-derived CaO by CO_2 immit method

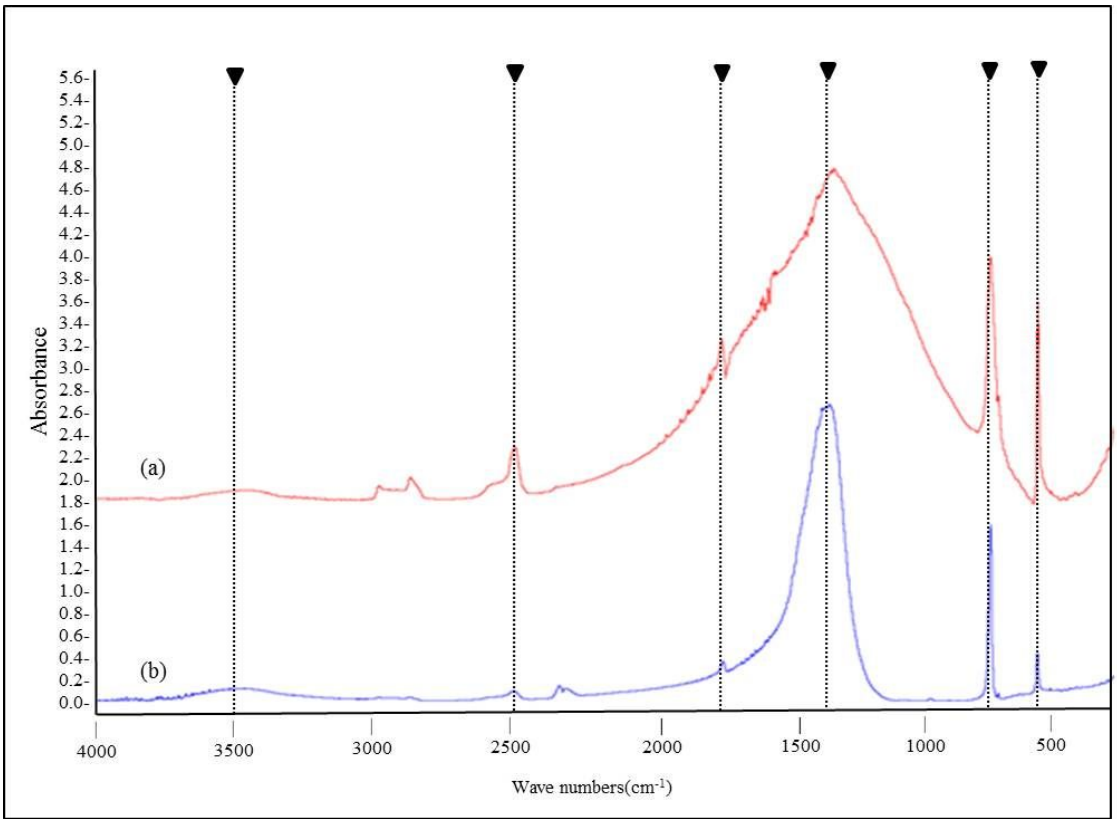

Figure 3. FT-IR analysis to verify the synthesis of $CaCO_3$ from abalone shell-derived CaO by CO_2 gas-infusing. Synthesized residues were performed FT-IR analysis, andthen compared with commercial $CaCO_3$ used as control to verify the synthesis of $CaCO_3$. (a) commercial $CaCO_3$, (b) $CaCO_3$ synthesized from abalone shell. As shown the Fig. 3, two peaks showed a similar tendency. Black arrow indicate the matching pick compared with commercial $CaCO_3$ used as control.

Ⅲ-C. Identification of optimize pH to synthesize the DCP from abalone shell-derived $CaCO_3$

The solution pH is very important for chemical reactions. Therefore, to identify the optimal pH fro synthesis of DCP from abalone shell-derived $CaCO_3$. The solution of calcium hydroxide was reacted with pH 6.02, pH 6.93 and pH 7.95 adjusted by 10% phosphoric acid. After reaction, each synthesized residues were performed FT-IR analysis and commercial DCP used as control ro identify the synthesis of DCP from abalone shell derived $CaCO_3$. As shown in Fig. 4, the pick of residue synthesized at pH 6.02 was completely mach with that of commercial DCP used as control. Our data are demonstratively that high purity of DCP was synthesized from abalone shell derived $CaCO_3$ by the reaction with phosphoric acid at pH 60.2.

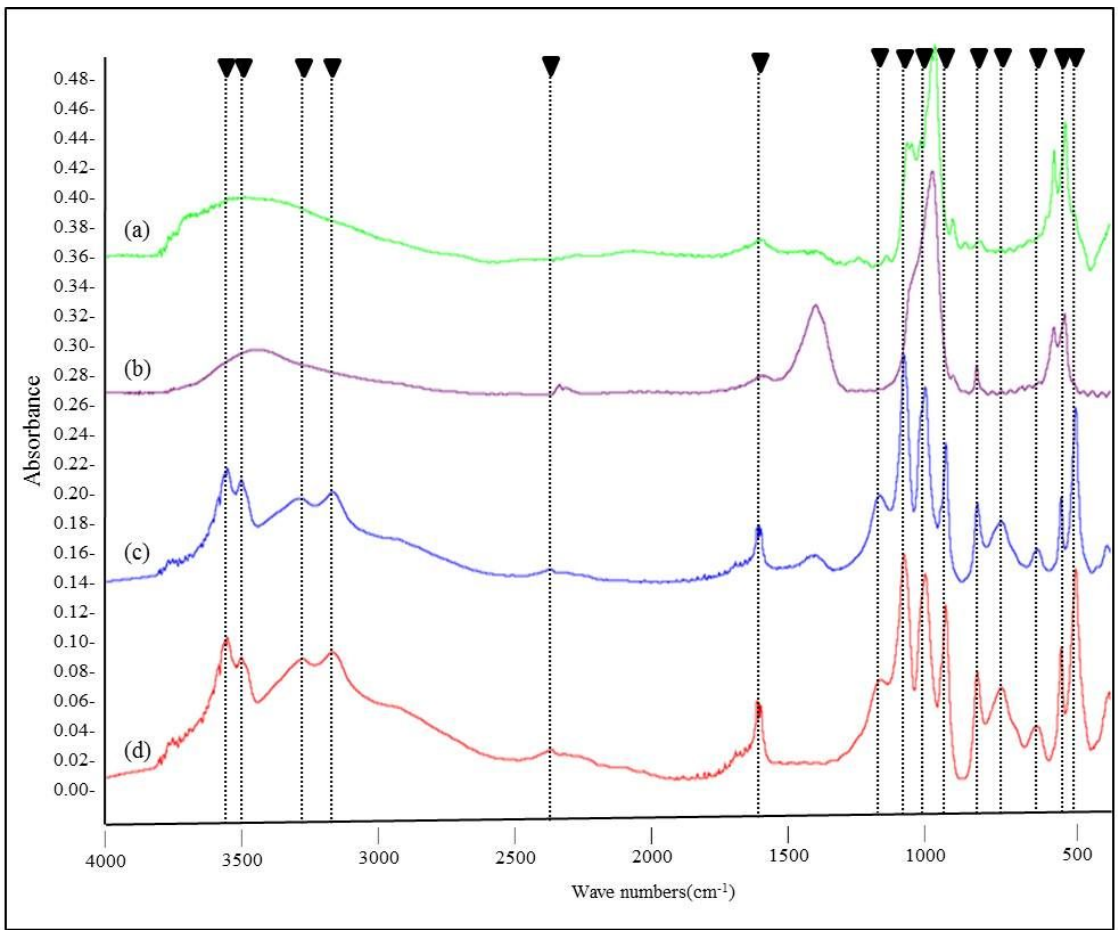

Figure 4. FT-IR analysis of DCP obtained at different pH to determine a valid pH. (a) commercial DCP, (b) DCP synthesized at pH 6.02, (c) DCP at pH 6.93 and (d) DCP synthesized at pH 7.95.

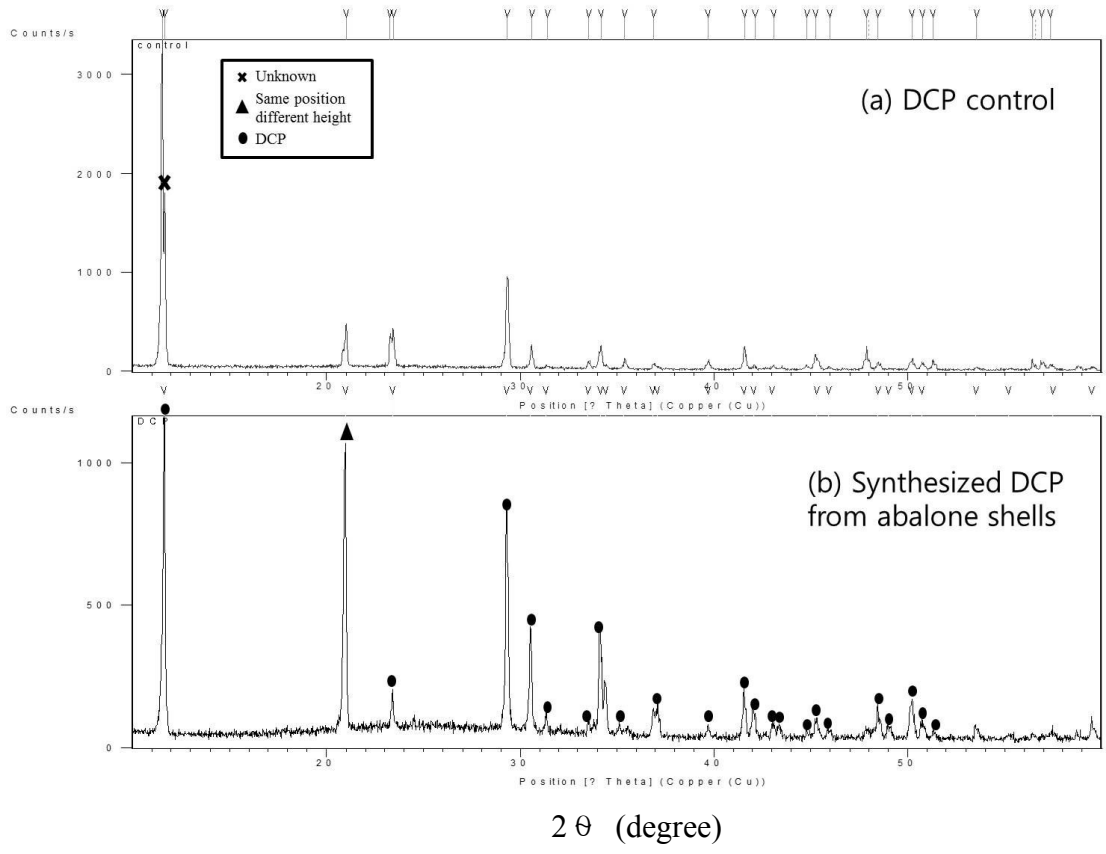

Figure 5. XRD analysis of DCP synthesized at 6.02 pH compared with control DCP. (a), the first peak was not observed in the control. (b), was observed at same position but with different heights. The other peaks were almost identical. These peaks indicated low crystallinity, similar to that of biological control DCP. The well defined peaks were assigned to the DCP substrate.

Ⅲ-D. Synthesis of β-TCP from abalone shell-derived DCP

The molar number of CaO needed to reaction a certain amount of DCP to become TCP, calculated with the chemical reaction formular, and then sintering at different temperature for synthesized β-TCP measured by FT-IR analysis.

To verify the optimize sintering temperature for the synthesis of β-TCP, abalone shell-derived DCP was tintered at different temperature (950℃, 1000℃, 1050℃ and 1100℃) with CaO by an electric furnace.

FT-IR spectrum of residues calcined at different temperature was obtained in the range of 400 - 4000 cm^{-1}. The FT-IR spectrum for the powders at various calcination temperature was shown in (Fig. 6). The peaks at 1030 and 570 cm^{-1} which attributed to PO_4^{3-}, indicating the presence of β-TCP phases. The C-O vibration in CO_3^{2-} vibration band disappeared and the septrum obtained was charcteristic of β-TCP. Fig. 7, shows XRD patterns of β-TCP synthesized by sintering at 1050℃. The XRD patterns β-TCP revealed three unknown peaks after sintering at 1050℃. The other peaks were almost identical. The β-TCP was synthesized successfully at 1050℃. Determination of β-TCP synthesized from abalone shell by the Korea Institute of Ceramic Engineering and Technology (Seoul, Republic of Korea) measured by XRD (Fig. 8).

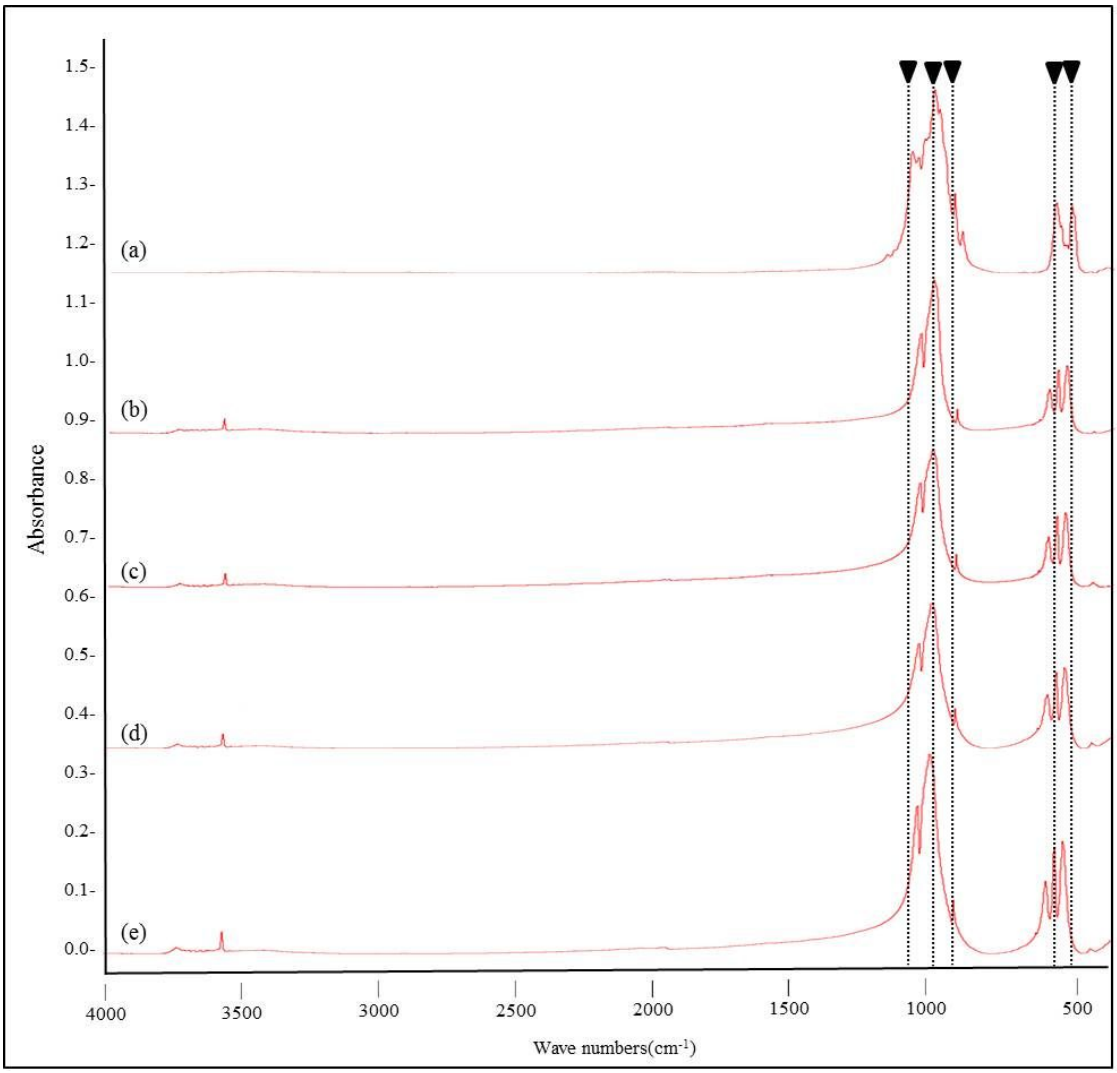

Figure 6. FT-IR analysis of β-TCP sintered at different temperatures to determine a valid sintering temperature. (a) commercial β-TCP, (b) calcined at 950℃, (c) 1000℃, (d) 1050℃ and (e) calcined at 1100℃. Black arrow indicate the matching pick compared with commercial β-TCP used as control.

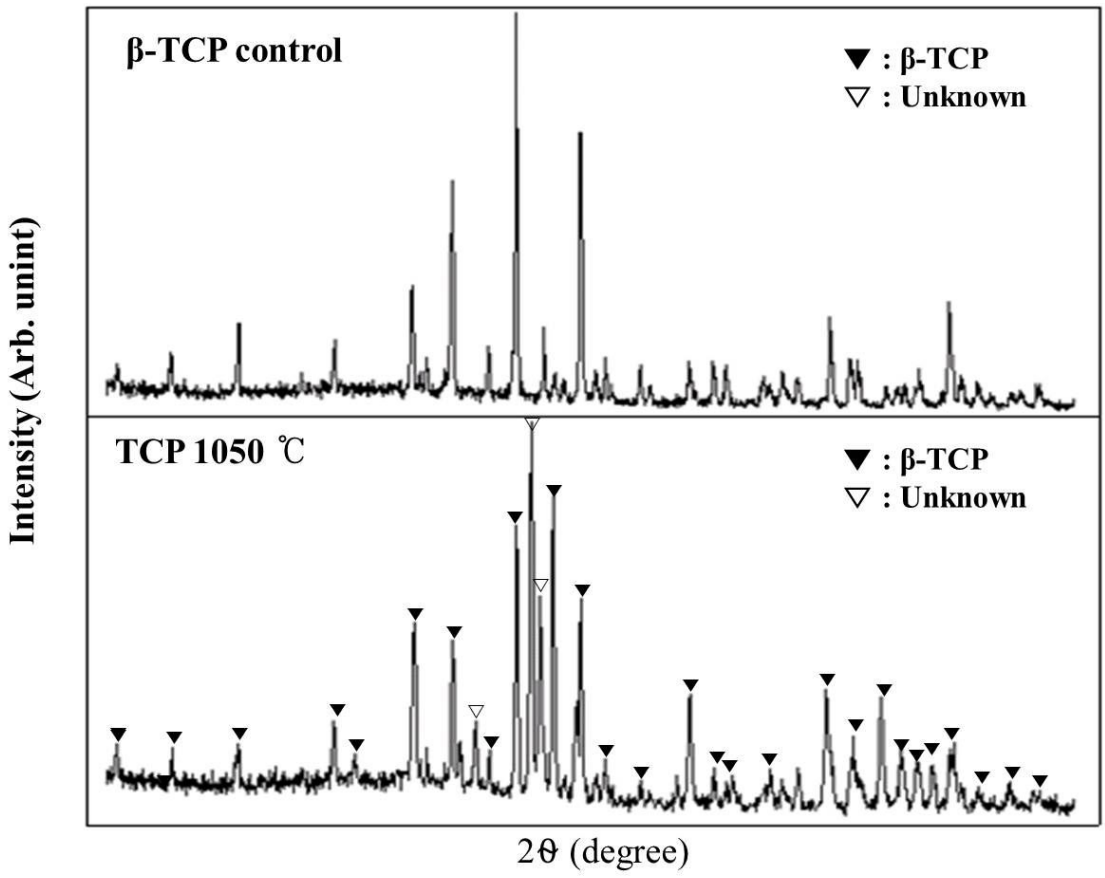

Figure 7. XRD analysis of the β-TCP synthesized from TCP sintered at 1050℃ compare with control β-TCP.

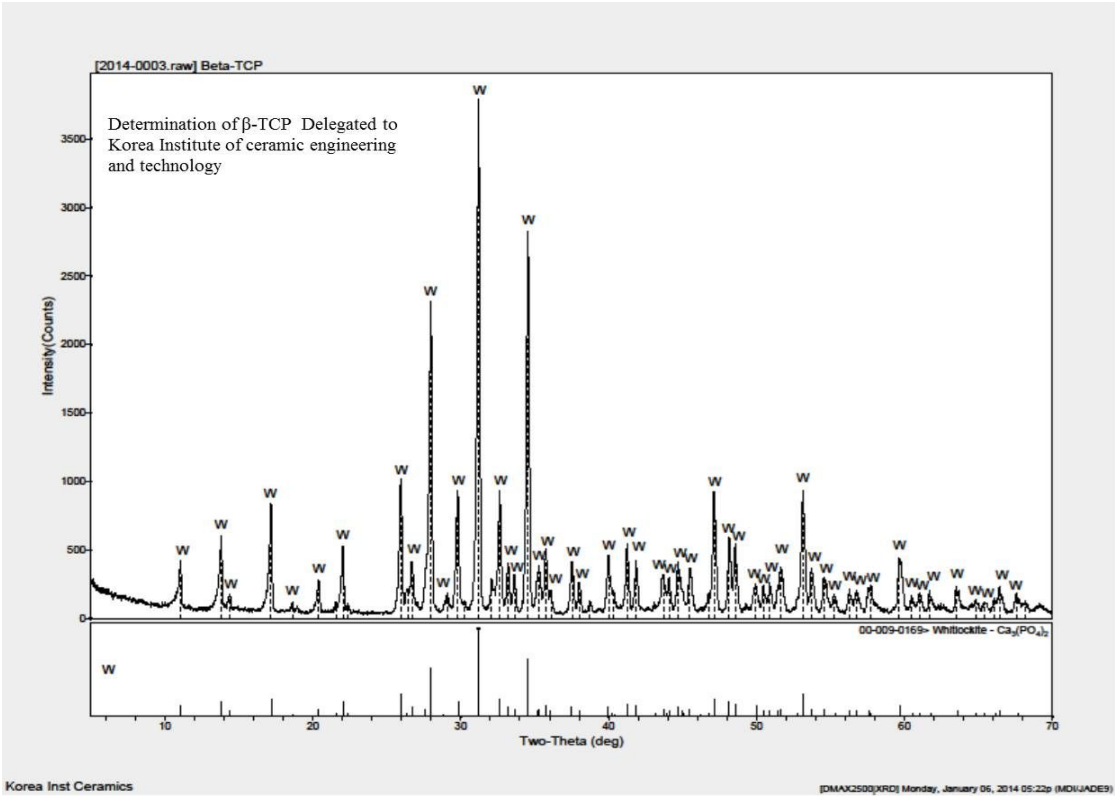

Figure 8. Reaffirmed of β-TCP synthesized from abalone shell by the Korea Institute of Ceramic Engineering and Technology (Seoul, Republic of Korea) measured by XRD.

Ⅲ-E. SEM images and EDS analysis of the β-TCP synthesized from abalone shell

After sintering at 1050℃, the surface appearance of a β-TCP sheet after sintering was observed by SEM at an acceleration voltage of 5.5 kV (Fig. 9). SEM revealed the β-TCP synthesized from abalone shell to have a flaky sheet morphology with a sheet size in the range of 20 - 40 μm. EDS was used for elemental analysis of the powder at a calcination temperature of 1050℃. EDS confirmed the presence of β-TCP, as shown in Fig. 10. Elemental analysis revealed O, P and Ca for calcium phosphates and confirming the purity of the sheet. EDS showed similar result to pure β-TCP, which was produced at 1050℃.

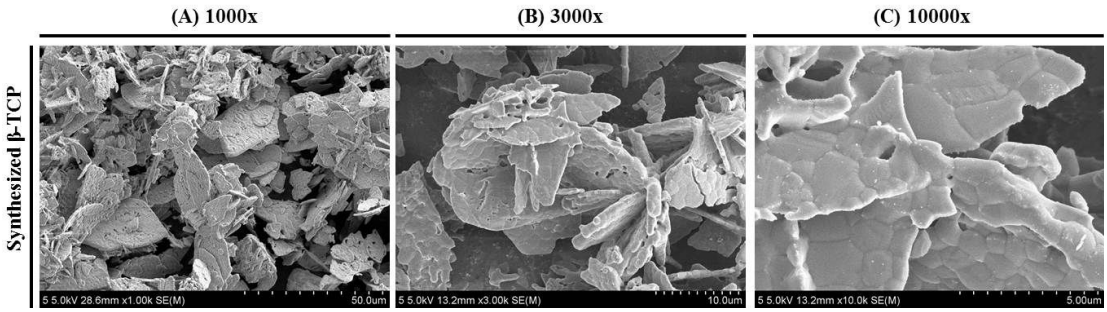

Figrue 9. SEM images showing surface appearance of β-TCP sheets. (A) 1000 x, (B) 3000 x, (C) 10000 x. The synthesized β-TCP sheets size average was approximately 200 μm.

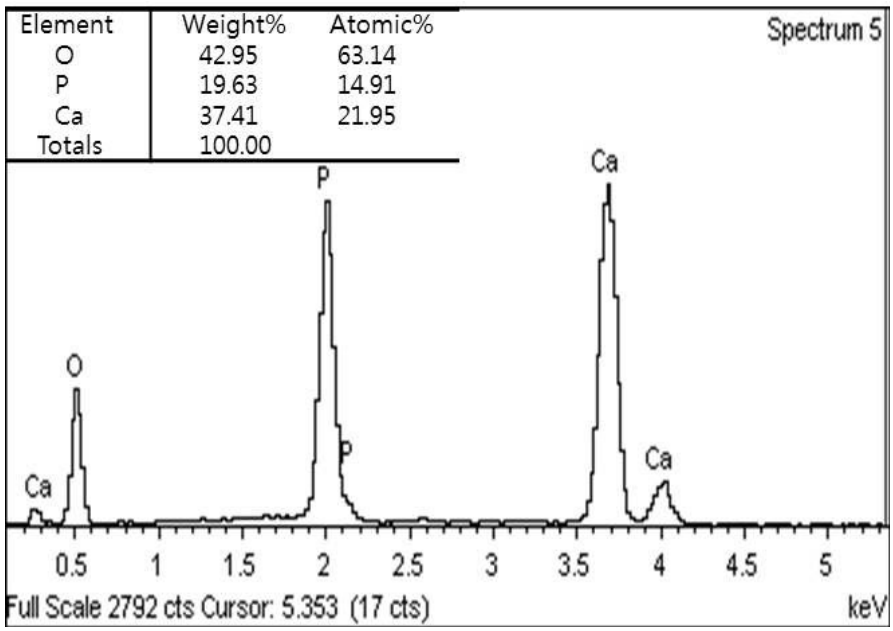

Figrue 10. EDS analysis of β-TCP synthesized from abalone shell. The β-TCP synthesized form abalone shell, the calcium to phosphorus ratio (Ca/P ratio) is 1.91.

Ⅲ-F. The cell cytotoxicity of β-TCP synthesized from abalone shell

The cell viability as one of biocompatibility assay by MTT assay. The eluents prepared by each eluents fo abalone shell-derived β-TCP did not affect the viability of hNOKs cells in presence or absence of serum. Furthermore, each eluents of abalone shell-derived β-TCP did not affect the viability of MG-63 cells.

There data are demonstrated that, abalone shell-derived β-TCP have a bilogical safety as the bioceramic to implant into body.

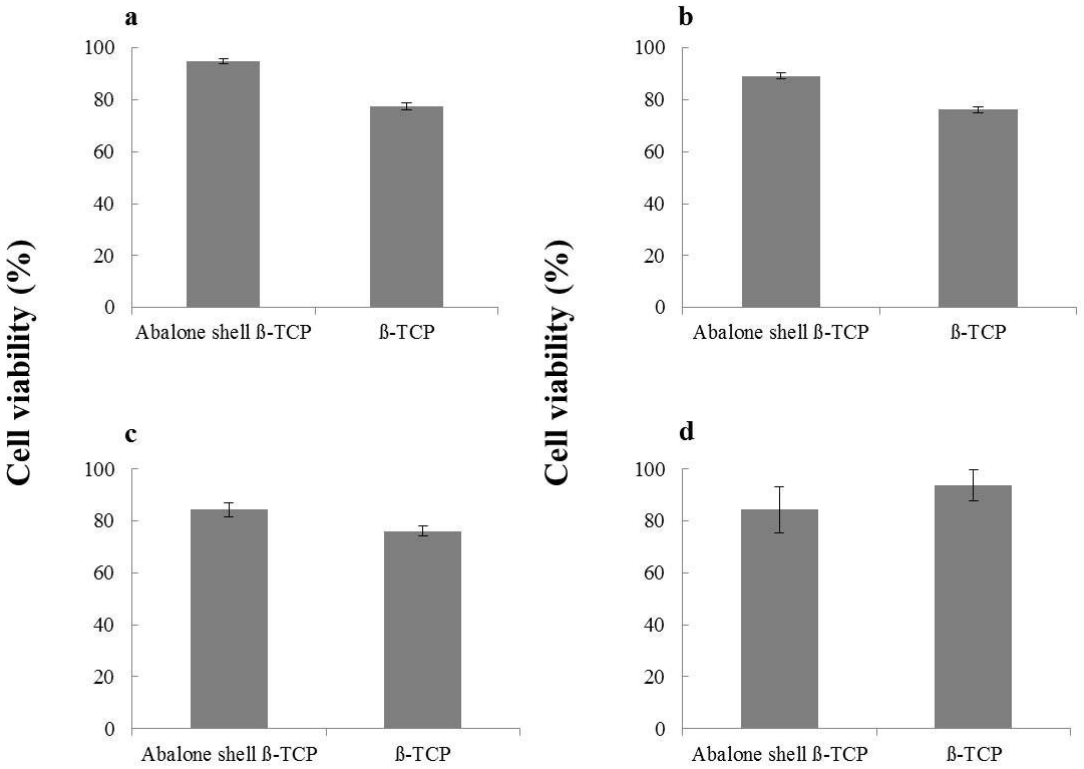

Figrue 11. Cell viability of β-TCP synthesized from abalone shell. Effluents of the control β-TCP and abalone shell β-TCP for measuring the cell cytotoxicity were prepared according to the guidelines provided by the Ministry of Food and Drug Safety (MFDS), Republic of Korea. a, HNOKs cultured in medium without 10% FBS, b HNOKs cultured in medium without 10% FBS. c MG-63 cell culrutred in medium without 10% FBS, d MG-63 cell cultured in medium without 10% FBS.

Ⅲ-G. Cell survival assay

To confirm the cell viability of abalone shell-derived β-TCP, we performed a cell survival assay to visualized both DAPI stain assay. As shown in Figure 12 (a), the commercial β-TCP as a control and abalone shell-derived β-TCP did not affect the cell survival on the MG-63 cells and hNOKs used as the normal cells.

Cell live and dead assay was performed to visualize the live (stained by green fluorescence) and dead cells (stained by red fluorescence) stained with green calcein AM and etidium bromide homodimer 1, respectively. As shown in Figure 12 (b), Both the MG-63 cells and hNOKs stimulated with the commercial β-TCP and abalone shell-derived β-TCP were stained green through the cleavage of the membrane permeable calcein AM by the cytosolic esterase in living cells. Otherwise, both the populations of MG-63 cells and hNOKs did not observed to stained red by ethidum bromide homodimer. These data demonstrated that abalone shell β-TCP was used in the manufacture as biocompatible material for bone grafting.

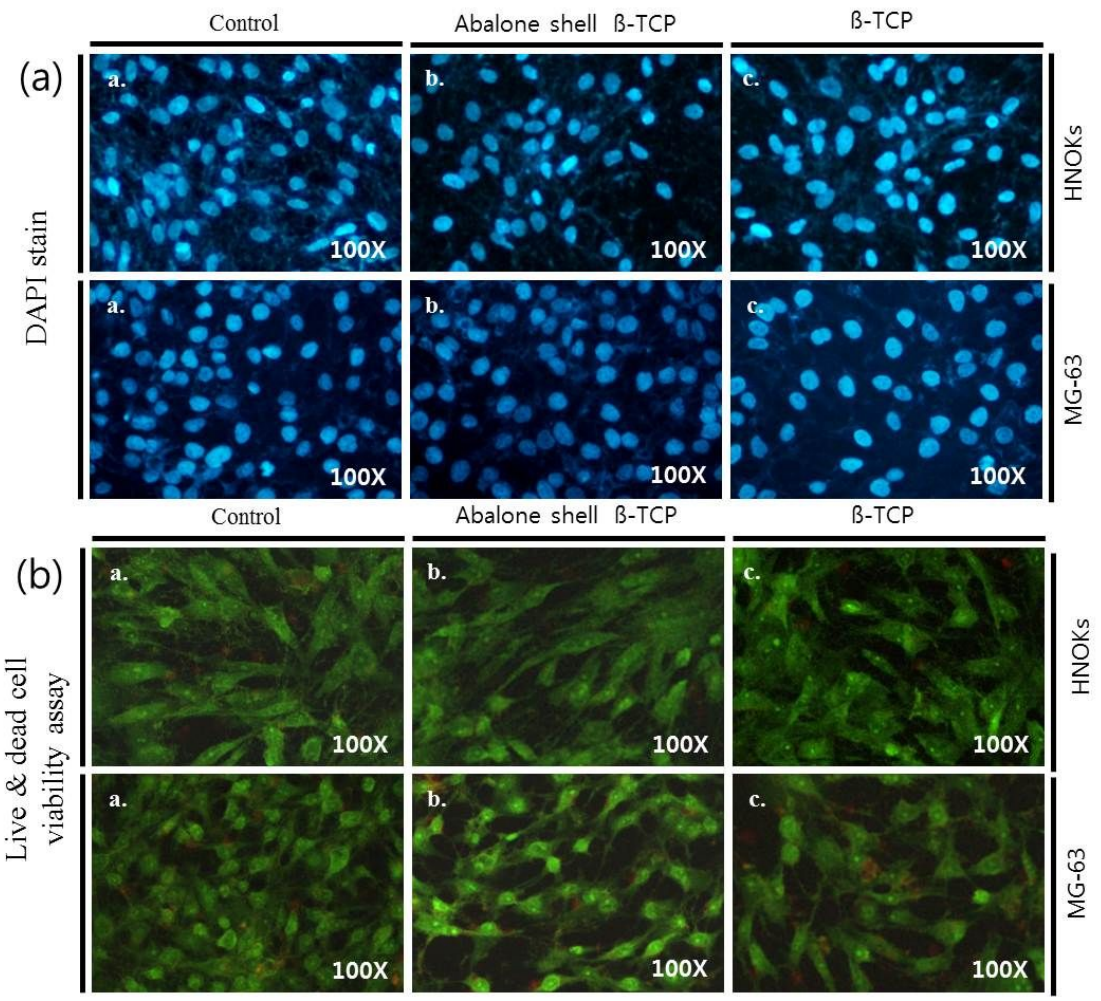

Figure 12. Comparison of cell survival between commercial β-TCP used as control β-TCP synthesized from abalone shell. Cell survival was performed by nuclear staining using DAPI (a) and Cell LIVE & DEAD assay (b). Life cells staining as green color, dead cells staining as red color.

Ⅳ. DISCUSSION

The biological mechanisms that provide a rationale for bone grafting are osteoconduction, osteoinduction and osteogenesis. Osteoconduction occurs when the bone graft material serves as a scaffold for new bone growth that is perpetuated by the native bone. Osteoinduction involves the stimulation of osteoprogenitor cells to differentiate into osteoblasts, which then begin new bone formation. Osteogenesis occurs when vital osteoblasts originating from the bone graft material contribute to new bone growth along with the bone growth generated via the other two mechanisms [40].

In thermal decomposition, amorphous calcium phosphate (ACP) or calcium deficient HA, which is obtained under neutral or acid conditions, is used for preparation. In the phosphorylated process, control by rigorous add phosphoric acid and the correct potential of hydrogen is used to synthesize pure TCP. Three polymorphs of TCP can be produced according to the sintering temperature: low-temperature β-TCP, and two high-temperature forms, α-TCP and ά-TCP. The last one has no practical use because it only exists at temperatures >1430℃ and reverts almost instantaneously to α-TCP upon cooling below the transition temperature. In contrast, β-TCP is stable at room temperature and transforms irreversibly to α-TCP at ~ 1125℃, which can be retained during cooling to room temperature [41-45]. Therefore, strict control of the sintering temperature is needed. Throughout the synthesis processes, each process to determine a valid sintering temperature. As results, a valid sintering temperature of CaO and β-TCP were 950℃ and 1050℃.

Bone graft materials such as β-TCP has been shown to conduct osteoblastic

differentiation and proliferation of bone marrow mesenchymal stem cells [44]. Calcium phosphate materials have been used increasingly in the past 40 years as bone graft substitutes in the dental and orthopedic fields. β-TCP powder was synthesized by using natural materials such as eggshells, cuttlefish bone and lyster shell had already studied. But, it is difficult to be recycled and these shells contain mass protein. Contrary, abalone shells were easy to recycled because of the vast majority of them are discarded as rubbish. And then, abalone shells contain very little of protein. So that, it is easily synthesis to high purity of biocompatible sorce as $CaCo_3$.

In this study, the synthesis behavior was dependent on the phosophoric acid, and the temperature for synthesis. The abalone shell powder was easily turned to CaO by sintering at 950℃ temperature. There are two major distinct phases of tricalcium phophate crystals: α-TCP and β-TCP. In spite of their similar chemical composition, their differet crystallographic features result in different resorption patterns. The α-TCP is obtained by heating above 1170℃ and is more soluble than β-TCP. In addition, β-TCP is more stable at room temperature than α-TCP, it presents higher solubility than HA and, consequently, can be degraded faster in the body, allowing a desirable gradual replacement by the newly formed bone [46-48].

Studies concerning β-TCP efficiency as a bone graft were already conducted. In vivo studies with β-TCP implanted in the rat femoral condyle were conducted by Kondo, et al., are repoted that β-TCP has a good biocompatibility, sinc both bioresorption and bone formation started at an early phase after implantation [49]. Furthermore, shiratori, et al., are report that also β-TCP an osteoconductive biomaterial, based on the histological and molecular fidings of bone tissue withdrawn from bone defects in rat femurs previously implanted with β-TCP

granules [50, 51]. In this context, the present work showed the synthesis β-TCP from natural material such as abalone shell. A biomaterial aiming to associate the osteoconductivity of β-TCP.

However, before performing in vivo studies on the impact of such material in bone tissue therapy, an in vitro evalution of cytocompatibility should be conduted. The FT-IR spectra exhibit the characteristic bands of CaO, $CaCO_3$ and DCP and β-TCP, at testing the accuracy of the biomaterial synthesis [52-54]. Lima,et al., are report that, assessed the number of biable balb/c3T3 fibroblasts after exposure to several metal-modified apatite extracts for 24 hr and concluded the cells respond to the metal that substitutes Ca or phosphate ions in the crystal lattice of HA. For that reson, soluble biomaterials such as metallic ion-substituted calcium phospates must be evaluated in terms of their cytocompatibility before clinical use. The CaO, $CaCO_3$, DCP and β-TCP synthesized from abalone shell of analysis the structure and morphology measured by SEM and XRD to determine. The MTT assay result shows that β-TCP are cytocompatible. Concerning the MTT assay result, considerable cell density was observed in the cells cultivated with effluents of control β-TCP and abalone shell β-TCP.

Comparison of cell survival cultured in control β-TCP and abalone shell β-TCP medium confirmed by DAPI staining and Cell Live & Dead assay. Assessment of cell survival in the samples used MG-63 and hNOKs cells. DAPI is a fluorescent stain that binds strong to A-T rich regions in DNA. It is used extensively in fluorescence microscopy. DAPI can pass through an intact cell membrane therfore it can be used to stain both live and fixed cells, though it passed through the membtane less efficiently in live cells and therefore the effectiveness of the stain is

lower. As the result, a majority of MG-63 and hNOKs cells were observed with blue-fluorescent. The Live & Dead assay stain solution is a mixture of two highly fluorescent dyes that differentially label live and dead cells. The live cell dye labels intact, viable cells green. The dye is membrane permeant and non-fluorescent until ubiquitous intracellular esterases remove the ester groups and render the molecule fluorescent. The dead cell dye labels the cells with a compromised plasma membrane red. This is membrane-mpermeant and binds to DNA with high affinity.

As shown in Fig. 12a, when cells die, their nuclei size decreases, which is shown as a higher intensity of DAPI from dead cells. Viable cells have very round and clear nuclei, whereas dead cells have smaller, condensed, cut or chopped nuclei. The control β-TCP and abalone shell β-TCP were the same as the control group. The live & dead viability/ cytotoxicity assay provided a two-color fluorescence cell viability assay based on the simultaneous determination of live and dead cells with two probes that measure the recognized parameters of cell viability intracellular esterase activity and plasma membrane integrity. As shown in Fig. 12b, the MG-63 and hNOKs cells in each group exhibited high cell viability and survival. Most of the cells were alive with almost no dead cells observed.

At present, many other studies have confirmed that biocompatible β-TCP was successfully synthesized by using natural materials such as eggshell and cuttlefish bone and oyster shell [55, 56]. However, many studies used complex process, high level concentration and several kind of acid to reaction. In this study, the basic raw material was used natural material as abalone shell for synthesized β-TCP. Afterwards, the abalone shell powder was easily turned to CaO By sintering process. The synthesis $CaCO_3$ was using CO_2 immit method. A phosphoric acid

was used as source of phosphor for the synthesis process. Therefore, the method of synthesized β-TCP from abalone shell was only using phosphoric acid and sintering process. As the FT-IR and XRD analysis results, the materials composition and crystalline were confirmed.

Finally, the beta tricalcium phosphate (β-TCP) synthesized by abalone shell are expected to a biocompatible material and mass product may be possible in the low cost and simple process.

Ⅴ. REFERENCES

[1] Breine. U and Branemark. PI, Reconstruction of alveolar jaw bone: An experimental and clinical study of immediate andpreformed autogenous bone grafts in combination with osseointegrated implants. Scand J Plastic Reconstr Surg Hand Surg. 1980; 14:23-48.

[2] Dahlin C, Linde A, Gottlow J and Nyman S. Healing of bone defects by guided tissue regeneration. J Plastic Reconstr Surg. 1988; 81:672-676.

[3] Dahlin C, Linde A, Gottlow J and Nyman S. Healing of maxillary and mandibular bone defects using a membrane technique an experimental study in monkeys. Scand J Plastic Reconstr Surg. 1990; 24:13-19.

[4] Schenk RK, Buser D, Hardwick WR and Dahlin C. Healing pattern of bone regeneration in membrane-protected defects: a histologicstudy in the canine mandible. Int J Oral Maxillofacial Implants. 1994; 9:13-29.

[5] Burchardt H. The biology of bone graft repair. Clin Orthop Relat Res. 1983; 174:28-42.

[6] Urist MR. Bone formation by autoinduction. Science. 1965; 150:893-899.

[7] AlGhamdi AS, Shibly O, Ciancio SG. Osseous grafting part II: xenografts and alloplasts for periodontal regeneration- a literature review. J Int Acad Periodontol. 2010; 12:39-44.

[8] Jensen OT, Adams MW. Anterior sinus grafts for angled implant placement for severe maxillary atrophy as an alternative to zygomatic implants for full arch fixed restoration: technique and report of 5 cases, J Oral Maxillofac Surg. 2014;

72:1268-1280.

[9] Calvo-Guirado JL, Garces M, Delgado-Ruiz RA, Ramirez Fernandez MP, Ferres-Amat E, Romanos GE. Biphasic β-TCP mixed with silicon increases bone formation in critical site defects in rabbit calvaria. Clin Oral Implants Res. 2014 (PMID: 24863557, Epub ahead of print)

[10] Tayapongsak P, Wimsatt JA, LaBanc JP, Dolwick MF. Morbidity from anterior ilium bone harvest: A comparative study of lateral versus medial surgical approach, Oral Surg Oral Med Oral Pathol. 1994; 78:296-300.

[11]. Clavero J, Lundgren S. Ramus or chin grafts for maxillary sinus inlay and local onlay augmentation : Comparison of donor site morbidity and complications, Clin Implant Dent RElat Res. 2003; 5:154-160.

[12] Einhorn TA. Enhancement of fracture-healing, J. Bone Joint Surg. Am. 1995; 77:940.

[13] Whitlock PW, Seyler TM, Parks GD, Ornelles DA, Smith TL, Van Dyke ME, Poehling GG. A novel process for optimizing musculoskeletal allograft tissue to improve safety, ultrastructural properties, and cell infiltration, J Bone Joint Surg Am. 2012; 94:1458-1467.

[14]. Emmings FG. Chemically modified osseous material for the restoration of bone defects, J. Periodontol. 1974; 45:385-390.

[15]. Wolff LF. Guided tissue regeneration in periodontal therapy, Northwest Dent. 2000; 79:23-28.

[16]. Rosenberg E, Rose LF. Biologic and clinical considerations for autografts and allografts in periodontal regeneration therapy, Dent Clin North Am. 1998; 42:467-490.

[17]. Froum SJ, Thaler R, Scopp IW, Stahl SS. Osseous autografts. I. Clinical responses to bone blend or hip marrow grfts, J. Periodontol. 1975; 46:515-521.

[18]. Mellonig JT. Autogenous and allogeneic bone grafts in periodontal therapy, Crit Rev Oral Biol Med. 1992; 3:333-352.

[19] Carmagnola D, Adriaens P, Berglundh T. Healing of human extraction sockets filled with Bio-oss, Clin,. Oral Impl. Res. 2003; 14:137-143.

[20] Mahesh L, Kotsakis G, Venkataraman N, Shukla S, Prasad H. Ridge preservation with the socket-plug technique utilizing an alloplastic putty bone substitute or a particulate xenograft: a histological pilot study. J Oral Implantol. 2013. (PMID:237728706, Epub ahead of print)

[21] Wenz B, Oesch B, Horst M. Analysis of the risk of transmitting bovine spongiform encephalopathy through bone grafts derived for bovine bone, Biomaterials. 2001; 22:1599-1606.

[22] Yeo SI, Park SH, Noh WC, Park JW, Lee JM, Suh JY. A comparative analysis of basic characteristics of several deproteinized bovine bone substitutes, Korean Academy of Periodontoloygy. 2009; 39:149-156

[23] Mantle D, Hardy MF, Lauffart B, McDermott JR, Smith AI, Pennington RJ.Biochem. Purification and characterization of the major aminopeptidase from human skeletal muscle, Biochem J. 1983; 211:567-573.

[24] Decheyne P, Groot K. In vivo surface activity of a hydroxyapatite alveolar boen substitute, *J. Biomed. Mater. Res.* 1981; 15:441-445.

[25] Orell F, The Rational Mechanics of Flexible or Elastic Bodies, 2000; 27:1638 - 1788.

[26] Lewandrowski. K, Gresser. JD, Wise DL and Trantolo DJ. Bioresorbable bone graft substitutes of different osteoconductivities, *Biomaterials.* 2000; 22:757-764.

[27] Klein CP, Driessen AA, de Groot K, van den Hooff A. Biodegradation behavior of various calcium phosphate materials in bone tissue, J Biomed Mater Res. 1983; 5:769-784.

[28] Orell F. Introduction to Leonhardi Euleri Opera Omnia, The Rational Mechanics of Flexible or Elastic Bodies, 2000; 27:1638-1788.

[29] Hench L. L. Bioceramics: from concept to clinic, Am. Ceram. Soc. 1991; 74:1487-1510.

[30] Thamaraiselvi T. V and Rajeswari S. Biological evaluation of bioceramic materials: a review, Trends in Biomaterials and Artificial Organs, 2004; 18:9-17.

[31] Guo LH, Li H, Gao XH. Phase transformations and structure characterization of calcium polyphosphate during sintering process, J. Mater. Sci.. 2004; 39:7041-7047.

[32] LeGeros RZ. Properties of osteoconductive biomaterials: calcium phosphates, Clin Orthop Relat Res 2002; 395:81-98.

[33] Comuzzi L, Ooms E, Jansen JA. Injectable calcium phosphate cement as a filler for bone defects around oral implants: an experimental study in goats, Clin Oral Implants Res 2002; 13:304-311.

[34] Brown WE, Chow LC. Combinations of sparingly soluble calcium phosphates in slurries and pastes as mineralizers and cements, US patent. 1986; 4:612-615.

[35] Stevenson S. Biology of bone grafts. Orthop Clin North Am. 1999; 30:543-552.

[36] Boyan BD, Ranly DM, Schwartz Z. Use of growth factors to modify

osteoinductivity of demineralized bone allografts: lessons for tissue engineering of bone. Dent Clin North Am. 2006; 50:217-228.

[37] Minichetti JC, D'Amore JC, Hong AY, Cleveland DB. Human histologic analysis of mineralized bone allograft (Puros) placement before implant surgery. J Oral Implantol. 2004; 30:74-82.

[38] Alcaide M, Serrano MC, Pagani R, Sánchez-Salcedo S, Vallet-Regí M, Portolés MT. Biocompatibility markers for the study of interactions between osteoblasts and composite biomaterials, Biomaterials. 2009; 30:45-51.

[39] Loosanoff V. L, Bernard I. J. Abalone, Collier's Encyclopedia. 1997; 1:6-8.

[40] Newman MG, Takei HH, Carranza FA. Implant Surgery and Bone Grafting Techniques. Carranza's Clinical Periodontology. 9th Edition. Saunders Co, USA 2002; 12:907-908.

[41] Buerger MJ. The rôle of temperature in mineralogy. Am Miner 1948; 33:101-121.

[42] Buerger MJ, Smoluchowski R, Meyer JE and Weyl WA. Crystallographic aspects of phase transformations. Phase transformations in solids. 1951; 1:183-211.

[43] Elliot JC. Structure and chemistry of the apatites and other calcium orthophosphates. Amsterdam: Elsevier Science; 1994.

[44] Dorozhkin SV. Calcium orthophosphate cements for biomedical application. J Mater Sci. 2008; 43:3028-3057.

[45] Kirk JF, Ritter G, Waters C, Narisawa S, Millán JL, Talton JD. Osteoconductivity and osteoinductivity of Nano FUSE(®) DBM. Cell Tissue Bank. 2013; 14:33-44.

[46] Barrère F, Van Blitterswijk CA, De Groot K. Bone regeneration: molecular and cellular interactions with calcium phosphate ceramics. Int J Nanomedicine. 2006; 1:317-332.

[47] Ducheyne P, Radin S, King L. The effect of calcium phosphate ceramic composition and structure on in vitro behavior. I. Dissolution. J Biomed Mater Res. 1993; 27:25-34.

[48] Kamitakahara M, Ohtsuki C, Miyazaki T. Review paper: behavior of ceramic biomaterials derived from tricalcium phosphate in physiological condition. J Biomater Appl. 2008; 23:197-212.

[49] Kondo A, Ogose A, Tokunaga K, Ito T, Arai K, Kudo N, et al. Bone formation and resorption of highly purified beta-tricalcium phosphate in the rat femoral condyle. Biomaterials. 2005; 26:5600-5608.

[50] Shiratori K, Matsuzaka K, Koike Y, Murakami S, Shimono M, Inoue T. Bone formation in beta-tricalcium phosphate-filled bone defects of the rat femur: morphometric analysis and expression of bone related protein mRNA. Biomed Res. 2005; 26:51-59.

[51] Gibson IR, Rehman I, Best SM, Bonfield W. Characterization of the transformation from calcium-deficient apatite to beta-tricalcium phosphate. J Mater Sci Mater Med. 2000; 12:799-804.

[52] Kumta PN, Sfeir C, Lee DHL, Olton D, Choi D. Nanostructured calcium phosphates for biomedical applications: novel synthesis and characterization. Acta Biomater. 2005; 1:65-83.

[53] Sader MS, Legeros RZ, Soares GA. Human osteoblasts adhesion and proliferation on magnesium-substituted tricalcium phosphate dense tablets. J Mater

Sci Mater Med. 2009; 20:521-527.

[54] Lima IR, Alves GG, Soriano CA, Campaneli AP, Gasparoto TH, Ramos ES Jr, et al. Understanding the impact of divalent cation substitution on hydroxyapatite: an in vitro multiparametric study on biocompatibility. J Biomed Mater Res A. 2011; 98:351-358.

[55] Lee YC, Characterisitics of Bio-Compatible Calcium Phosphates Fabricated by Natural Materials, Mokpo national university (2009).

[56] Kwon MD, Oh SH and Lee SJ, Synthesis of β- tircalcium Phosphate by Using an Eggshell, Mokpo national university (2002).

감사의 글

먼저 논문이 있기까지 12년간 저에게 갈 길을 이끌어 주시고 항상 깊은 사랑과 믿음으로 지켜주신 존경하신 아버지, 어머니, 4년 남짓한 유학 생활동안 모든 면에서 챙겨주시고 걱정해주시고 학문의 길을 이끌어주신 존경하는 김 수 관 지도교수님께 깊은 감사를 드립니다. 그리고 사랑하는 이숙영 교수님, 표현할 수 없을 정도로 절 챙겨주시고 항상 고민에 빠져있고 나태해지고 힘들어 할 때 곁에서 늘 격려해 주시고 아껴주신 김재성 교수님께 평생 감사한 마음으로 가슴속 깊이 기억하며 살겠습니다. 그리고 중국에 계시는 우리 방현호 교수님께 깊은 감사를 보내 드립니다.

그 외에 제의 곁에서 항상 힘이 되어주시고 활력소가 되어 주신 모든 분께 감사 합니다.

어려서부터 저를 바른길로 이끌어주시고 인생의 도리를 가르쳐 주신 송학예 외할머니, 김규영 큰 외삼촌, 저를 제일 이뻐라하신 김규훈 둘째 외삼촌, 저랑 친구처럼 대해주시는 김규무 작은 외삼촌 그리고 홍선희 둘째 어머니, 마봉화 작은 어머니 모두 감사 드립니다. 나와 함께 한국에서 4년 남짓이 동거동락한 정면진,

내 짱친 김광택, 나에게 활력소가 되어준 전현수, 나의 튼튼한 후원자이자 내 친동생과 나름없는 김설봉 동생, 너의들이 있어서 너무 힘이 되었습니다.

본 논문이 있기까지 심사해주시고 늘 도와주진 기초의학과 김재성 교수님, 이숙영 교수님, 구강악안면 외과 오지수 교수님, 문성용 교수님, 유재식 교수님, 병리생리학과 임성철 교수님, 서울대학교 구강악안면외과학 이종호 교수님께 감사드립니다.

그리고 석. 박사 학위과정동안 늘 함께 했던 친구처럼 형님처럼 항상 챙겨준 승찬이, 선후배인 변주희 석사님, 장은숙 선생님, 나의 첫 후배이자 곁에서 동생처럼 따뜻하게 챙겨준 임민지 석사님, 석사학위 과정인 우리 방장님 오다혜, 친 동생이고픈 강경록, 연구원 생활을 열심히 하고 있는 김복희, 조인아 그리고 실험실 분위기 메이커인 장현정 선생님, 실험실 막내인 신나라, 우리 실험시에서 항상 함께 실험하면서 한 식구처럼 지내고 있는 박보람, 장재곤 선생님, RIC의 맞형님 박상연형님, 첨엔 어색했지만 함께 지내면서 친해진 이가영 선생님, 김은경 선생님, 황유의 선생님... 함께 했던 시간들이 너무 소중하고 평생 함께 했었던 소중한 추억들을 영원히 잊지 못할 것 같습니다.

그리고 유학생활 4년 넘게 하면서 친 형님처럼 대해주신 구강악 악안면 외과 레지던트 임형섭 형님, 김문섭 형님, 진수영 형님 너무 고맙고 항상 마음속 깊이 기억하겠습니다.

그리고 늘 따뜻하게 대해주신 국중기 교수님, 웃는 모습이 매력적이신 김도경 교수님, 너무 멋지신 김춘성 교수님과 차도남 문성민 박사님... 항상 격려해주시고 도와주심에 많은걸 배웠습니다. 감사합니다.

이젠 새로운 시작으로 새로운 도전이 시작 되었습니다. 항상 더 많은 학문을 배워 나가고 두려움 없이 도전하는 그런 사람으로 되어가도록 한 걸음, 한 걸음 천천히 걸어가도록 하겠습니다. 감사 합니다.